Multi-Fidelity Multi-Objective Optimization of Electric Machines Having Heterogeneous and Blocked Evaluation Times

Balija Santoshkumar *Student Member, IEEE*, and Kalyanmoy Deb, *Fellow, IEEE*

***Abstract*—Complex engineering design problems often involve multiple objectives and constraints, requiring third-party simulation software based evaluations having heterogeneous computational times. For a time-budget optimization run, a judicious management of high-fidelity evaluations of computationally cheaper and expensive objectives and constraints must be adopted. In this paper, we apply a recently proposed multi-fidelity selection based evolutionary multi-objective optimization (EMO) procedure to optimize an electric machine design problem to demonstrate its effectiveness in solving real-world computationally expensive optimization problems. The problem formulation follows that presented in a foundational study, with appropriate modifications to align with objectives and constraints of the current application. With commercial multi-physics expensive evaluation of electromagnetic and structural analysis softwares, and cheaper mathematical expressions, we demonstrate how the proposed MFE-NSGA-III approach can be efficiently applied to find a number of alternate trade-off designs compared to a conventional surrogate-assisted optimization procedure. The proposed procedure judiciously assigns computationally cheaper and expensive blocked objectives/constraints adaptively to make the overall procedure more computationally effective.**

I. Introduction

Electric machines are critical components across numerous industries, including automotive, aerospace, renewable energy, and industrial manufacturing, making their optimal design increasingly important for improving energy efficiency, performance, and sustainability [1], [2]. The design of electric machines involves balancing multiple conflicting objectives and satisfying various constraints, often requiring careful consideration of electromagnetic, thermal, mechanical, and structural aspects [3].

Several studies have addressed electric machine design optimization, focusing on aspects such as maximizing torque output, minimizing torque ripple, reducing weight for improved power density, enhancing efficiency, and managing mechanical stress and thermal properties [4]. Traditional design approaches often rely on iterative trial-and-error methods or simplified analytical models, which may not adequately capture the complex interactions between design parameters and performance metrics. More recently, evolutionary multi-objective optimization (EMO) algorithms have emerged as powerful tools for exploring the design space and identifying trade-off solutions that satisfy multiple conflicting objectives simultaneously [5]–[7]. A recent competition of electric motor design attracted a number of researchers world-wide to address an electric motor design task [8], [9].

Despite all these efforts, the analysis required for design optimization of electric machines remains a computationally challenging task. High-fidelity evaluation of candidate designs typically requires finite element analysis (FEA) for electromagnetic performance assessment and structural analysis for mechanical integrity verification. These simulations can be computationally expensive, with evaluation times ranging from minutes to hours per design, depending on the model complexity and desired accuracy. When coupled with population-based optimization algorithms that require hundreds to thousands of total solution evaluations, the total computational cost can become prohibitive for practical design scenarios with limited time budgets. To address this challenge, surrogate-assisted evolutionary multi-objective (SA-EMO) optimization approaches [10]–[16] have evolved as powerful techniques that approximate expensive simulations with fast-to-evaluate surrogate models. However, most surrogate-assisted methods do not consider heterogeneous evaluation times across objectives and constraints; they evaluate all objectives and constraints for a particular selected solution at high fidelity, resulting in unnecessary high-fidelity evaluations of objectives and constraints which may not provide useful additional information. This challenge is further compounded when different objectives and constraints require evaluations using different simulation tools with heterogeneous computational times, necessitating intelligent strategies for managing computational resources during the optimization process. Recently, several studies have emerged to address the heterogeneous evaluation time issue [17]–[23].

While these existing methods provide frameworks for handling heterogeneous evaluations, their application to electric machine design remains limited. Khoshoo et al. [24] recently proposed a surrogate-assisted optimization approach specifically for electric machines, though their work did not fully exploit the heterogeneous nature of electromagnetic, structural and block evaluation of objectives and constraints. In this paper, we extend their work by incorporating an additional structural stress analysis component which is more important for mechanical integrity and exploring the design optimization using multi-fidelity evolutionary multi-objective

Balija Santoshkumar is with the Department of Mechanical Engineering, Michigan State University, East Lansing, MI, 48824 USA e-mail: balijasa@msu.edu.

Kalyanmoy Deb is with the Department of Electrical and Computer Engineering, Michigan State University, East Lansing, MI, 48824 USA email: kdeb@msu.edu.

optimization (MFE-EMO) [23]. The multi-fidelity approach allows for judicious allocation of computational resources by selectively assigning high-fidelity evaluations only when necessary, while using faster lower-fidelity approximations for preliminary screening and exploration of the design space.

In the remainder, we present the electric motor design problem formulation as a bi-objective optimization problem in Section II. Evaluation procedure of a solution using electromagnetic and structural analysis softwares are briefly discussed in Section III. Since different objectives and constraints use different evaluation times and they are computationally expensive at different scales, a surrogate-assisted optimization procedure is adopted based on a recently proposed mixed-fidelity evaluation based algorithm, which is described briefly in Section IV. Thereafter, in Section V, we provide results without and with the stress constraint. Since both objectives – maximization of torque and minimization of torque ripple – are evaluated using the same electromagnetic analysis software, we demonstrate how MFE-EMO can handle a blocked evaluation scenario. Finally, Section VI concludes the study.

II. Problem Formulation

The objective of this work is to optimize the design of an interior permanent magnet (IPM) electric machine by achieving a desirable trade-off between multiple conflicting performance metrics. Specifically, the optimization aims to maximize the average electromagnetic torque while minimizing the torque ripple, subject to ten geometric constraints [24] and an additional stress constraint.

A. Design Variables

The design (decision) variables and their corresponding bounds, adopted from [24], are listed in Table I and described in Figure 1.

TABLE I: Design variables and their limits.

x_i	Variable description	Unit	$x_i^{(\mathrm{ref})}$	$x_i^{(L)}$	$x_i^{(U)}$
x_1	Height of rotor pole cap	mm	9.56	7.65	11.47
x_2	Magnet thickness	mm	7.16	5.73	8.59
x_3	Magnet width	mm	17.88	14.30	21.46
x_4	Angle between magnets	degree	145.35	116.28	174.42
x_5	Bridge height	mm	1.99	1.59	2.39
x_6	Q-axis width	mm	13.90	11.12	16.68
x_7	Slot height	mm	30.90	24.72	37.08
x_8	Slot width	mm	6.69	5.35	8.03
x_9	Height of slot opening	mm	1.22	0.98	1.46
x_{10}	Width of slot opening	mm	1.88	1.50	2.26

Each design evaluation requires an electromagnetic analysis (EMA) simulation, making the optimization process highly computationally expensive. The MFE-EMO framework [23] is employed to address this challenge by using mixed-fidelity evaluations combining high-fidelity simulations with faster surrogate-assisted or low-fidelity models to accelerate convergence without compromising accuracy.

B. Objectives and Constraints

The bi-objective optimization problem is formulated as:

$$\begin{array}{lll} \text{Maximize} & f_1(\mathbf{x}) = T_{\text{avg}}(\mathbf{x}), & \text{(Average Torque)} \\ \text{Minimize} & f_2(\mathbf{x}) = T_{\text{ripple}}(\mathbf{x}), & \text{(Torque Ripple)} \\ \text{subject to} & g_j(\mathbf{x}) \leq 0, \ j = 1, \ldots, J, & \end{array} \quad (1)$$

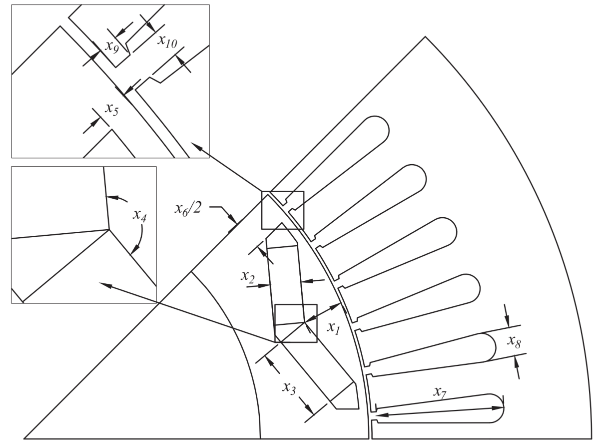

Fig. 1: Schematic illustration of the electric machine geometry showing the design variables listed in Table I, reproduced from Khoshoo et al. [24].

where $\mathbf{x}$ represents the vector of design parameters. The constraints $g_j(\mathbf{x})$ represent geometric constraints to ensure manufacturability, mechanical integrity, and electromagnetic feasibility of the motor design [24]. The description and formulation of these 10 geometric constraints are provided in [24]. In addition, a stress constraint is imposed to ensure that the maximum von Mises stress at 8,000 RPM speed does not exceed 350 MPa, thereby maintaining structural safety of the rotor. Two sets of optimization results are analyzed: one considering only geometric constraints and another including the additional stress constraint, allowing for assessment of how structural limitations influence the optimal performance trade-offs. The latter study creates three levels of computational fidelity with blocked evaluation to adequately test the proposed MFE procedure [23].

This problem serves as a representative example of a real-world engineering design task characterized by expensive evaluations and complex trade-offs. The proposed MFE-EMO framework [23] enables efficient exploration of the design space by selectively using mixed-fidelity evaluations, thereby significantly reducing computational cost while maintaining the quality of the obtained Pareto-optimal set.

III. Evaluation Using Electromagnetic and Structural Analysis

This section describes the automated workflows used for electromagnetic and structural analysis of rotor designs. Both analyses are driven by Python scripts that interface with commercial simulation tools: Altair Flux® [25] for electromagnetic evaluation and Altair SimLab® [26] for structural analysis.

A. Electromagnetic Analysis Setup

The electromagnetic analysis was conducted using Altair Flux software. The automated process involves the following key steps:

- **Input:** A baseline flux model and geometry information are provided as inputs.

- **Geometry Update and Solving:** The workflow performs three tasks:
  1) Updates the geometry based on new decision variables,
  2) Generates the mesh, and
  3) Executes the electromagnetic solver.
- **Output:** The outputs include mean torque, torque ripple, and the final rotor geometry exported as a `.fem` file.

Figure 2 shows the obtained flux distribution using the automated workflow implemented.

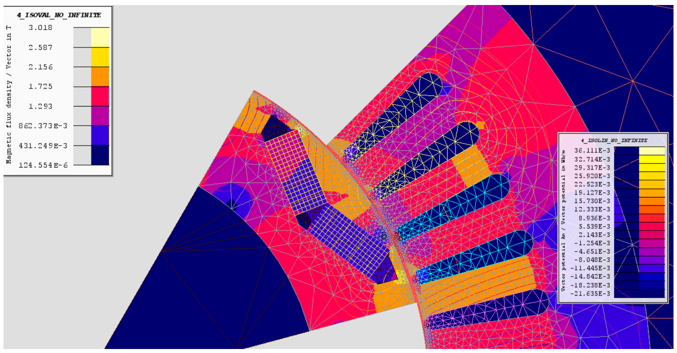

Fig. 2: Automated workflow for electromagnetic analysis using Altair Flux software.

B. Structural Analysis Setup

The structural analysis was conducted using Altair SimLab, again automated via Python scripting. The `.fem` file obtained from the electromagnetic analysis serves as the input to the structural analysis code. The analysis workflow consists of the following steps:

- **Input:** Rotor geometry imported from the electromagnetic analysis as a `.fem` file.
- **Preprocessing and Solving:** The Python script carries out the following tasks:
  1) Assigns material properties,
  2) Applies loads (rotational speed),
  3) Applies boundary conditions,
  4) Defines contacts, and
  5) Initiates the solver for structural evaluation.
- **Output:** The key output is the maximum stress value experienced by the rotor under specified operating conditions.

Figure 3 shows the obtained stress distribution using the implemented automated workflow for a typical rotor design.

IV. Multi-Fidelity Surrogate-Assisted Optimization Approach

In this section, we briefly describe the MFE-EMO [23] approach implemented to solve the design optimization of the electric machine. MFE-EMO selectively evaluates objectives and constraints at high fidelity based on their probability of being non-dominated, extent of constraint violation, surrogate model uncertainty, and evaluation time. Unlike traditional surrogate-assisted methods that evaluate all objectives and

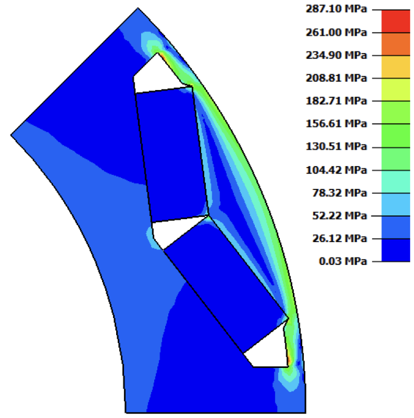

Fig. 3: Automated workflow for structural analysis using Altair SimLab.

constraints when a solution is selected for high-fidelity evaluation, MFE-EMO employs a mixed-fidelity evaluation strategy that can evaluate different objectives and constraints independently. This is particularly advantageous for electric machine design optimization where electromagnetic FEA, geometric constraints, and structural FEA have heterogeneous computational costs and torque and torque ripple evaluated through the same third party software, facilitating block evaluation.

The algorithm starts with constructing surrogate models for each objective and constraint function using an initial design of experiments. We use the same Kriging-based surrogate models as in [23], where full training and update details are provided. At each generation, it determines which specific objectives and constraints of which solutions should be evaluated at high fidelity using a mixed-fidelity survival selection (MFS):

Step 1: Solution classification. First, every population member s is classified based on a feasibility metric

$$Z_s^j = \frac{-\mu_s^j}{\sigma_s^j}, \tag{2}$$

where μ_s^j and σ_s^j are the predicted constraint value and associated surrogate uncertainty for constraint j of solution s. A solution is classified as Class I (feasible) if $\min_{j=1}^{J} Z_s^j \geq -e$. Remaining solutions are classified as Class II (infeasible).

Step 2: Class I population exceeds N. When the number of Class I solutions exceeds the population size N, a mixed-fidelity selection (MFS) metric ρ_s^m is used for every objective (m) of every feasible solution (s):

$$\rho_s^m = \left(1 + \widehat{ET}_m\right)^{\alpha} P_s^m \left(1 + \left(\frac{\sigma_s^m}{|\Delta f_m|}\right)^{1/\eta}\right), \tag{3}$$

where P_s^m is the probability of solution s being non-dominated for objective m among its neighbors (in the sense of reference vectors), σ_s^m is the surrogate prediction uncertainty, Δf_m is the range of the m-th objective in the population, $\widehat{ET}_m$ is the normalized evaluation time for objective m, and α is adaptively updated based on elapsed computational time to emphasize cheaper evaluations early in the search and more expensive ones later [18], [20], [23]. The parameter η controls the influence of surrogate uncertainty.

For each reference vector, the solution with the highest ρ_s^m value is selected. For this solution, only constraints close to their boundaries ($e \leq Z_s^j \leq -e$) are marked for high-fidelity evaluation; constraints clearly satisfied ($Z_s^j > -e$) are not evaluated. At least one critical objective per solution undergoes high-fidelity evaluation.

Step 3: Class I population less than N, but more than zero. When the number of Class I solutions is at least one but less than N, all Class I solutions are included in the next generation population P_{t+1}, with their critical objectives and near-boundary constraints evaluated at high fidelity as in Step 2. The remaining population slots are filled with Class II solutions having the highest probability of overall constraint satisfaction (PG_s), but these infeasible solutions receive no high-fidelity evaluations as they are unlikely to lead to optimality.

Step 4: All solutions infeasible. When all solutions are infeasible (Class I is empty), the solution with the highest PG_s value (least overall constraint violation) is chosen, and only its least-violated constraint is evaluated at high fidelity. No objectives are evaluated in this case.

This selective evaluation strategy allows MFE-EMO to judiciously allocate the computational budget by avoiding unnecessary expensive evaluations of constraints for highly feasible or highly infeasible solutions, and objectives for infeasible solutions. The approach has been particularly promising for real-world optimization problems involving heterogeneous evaluation costs. Specifically, the electric machine design optimization problem considered here involves computationally expensive objectives and constraints with heterogeneous evaluation times, where objectives torque and torque ripple come from the same third-party software (Altair Flux), constituting block-evaluation objectives. This makes MFE-EMO particularly interesting for the problem considered here, as it can exploit both the heterogeneous evaluation times and the block-evaluation structure to achieve better convergence with the same computational budget compared to traditional approaches that evaluate all objectives and constraints.

V. Results

In this section, we present results of electric machine design optimization with and without stress analysis under different evaluation time scenarios, comparing the performance of SA-NSGA-III and MFE-NSGA-III. In SA-NSGA-III, updated surrogates are used for optimization at every generation, but once a solution is selected for high-fidelity evaluation, all objectives and constraints are high-fidelity evaluated. For all cases, a population of size (N) 50 and the number of reference directions same as the population size (N) are chosen. The overall time budget of $T_{\max}$ is set as 300, and the initial design of experiments (DoE) N_{DoE} is set as 50. The surrogate generations (t_S) to create offspring population Q_{t+t_S} is set as 20 for all cases. Due to the high computational cost of each optimization run, each involving hundreds of Altair Flux and SimLab evaluations and requiring approximately a day of computation, results are reported from a single run per configuration. The parameter η in Eq. 3 for handling surrogate error is set to 20, based on an earlier study [18].

A. Results Without Stress Constraint

This section presents the optimization results obtained by considering only the geometric constraints. The outcomes highlight the trade-off between average torque and torque ripple. The parameter e in the MFE-EMO framework [23] is set to $e = -2$. Figure 4 shows the final-generation solutions obtained under two evaluation-time (ET) configurations: one with ETs = ($\boxed{0.5,\ 0.5}$ | 0.05, 0.05, . . ., 0.05) and another with ETs = ($\boxed{0.99,\ 0.99}$ | 0.001, 0.001, . . ., 0.001). Here, blocked objectives (evaluated together) are shown in boxes and the separator | distinguishes objectives from constraints. The configuration with relatively cheaper objective evaluation times compared to constraint evaluation times allows the MFE-EMO algorithm to run for more iterations and achieve a better spread of the Pareto front, but with higher average torque values. Since torque maximization is more challenging [24], additional iterations with the cheaper objective evaluation time helps find better torque solutions. The corresponding number of high-fidelity evaluations recorded for this configuration is shown in Figure 5. These results show that MFE-EMO attains better performance by performing an unequal number of solution evaluations and prioritizing the most important objectives and constraints, effectively balancing solution quality and computational efficiency with the proposed framework.

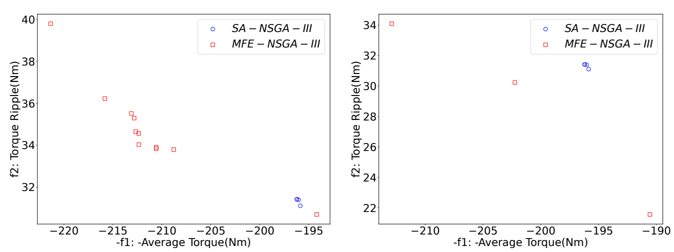

(a) ETs = ($\boxed{0.5,\ 0.5}$ | 0.05, 0.05, . . ., 0.05).

(b) ETs = ($\boxed{0.99,\ 0.99}$ | 0.001, 0.001, . . ., 0.001).

Fig. 4: Comparison of final generation feasible solutions under two different ET configurations. Relatively higher computational time (Fig. 4b) for objectives causes better torque ripple solutions at the expense of average torque values.

B. Results With Stress Constraint

This section presents the optimization results when the additional stress constraint (maximum von Mises stress ≤ 350 MPa at 8000 RPM) is incorporated. These results show how structural limitations influence the achievable torque and torque ripple. In this case, the parameter e in the MFE-EMO framework [23] is set to $e = -4$ to emphasize more evaluations of the stress constraint, as it is highly critical and modeled using surrogate approximations. Figure 6 shows the final-generation non-dominated solutions, where we can see that MFE-NSGA-III achieves superior performance compared to

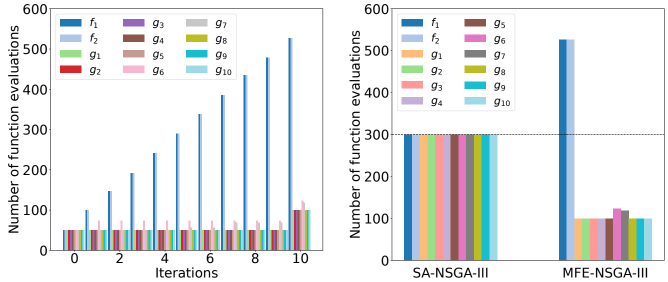

(a) Number of hi-fi evals per iteration for MFE-NSGA-III.

(b) Total no. of hi-fi evals for SA-NSGA-III and MFE-NSGA-III.

Fig. 5: Number of hi-fi evaluations recorded using SA-NSGA-III and MFE-NSGA-III with ETs ($\boxed{0.5,\ 0.5}\,|\,0.05, 0.05, \dots, 0.05$).

SA-NSGA-III. Figure 7 presents the HV comparison between both algorithms. The solutions from both algorithms were combined to compute common ideal and nadir points, given by $z^* = (-204.91,\ 13.51)$ and $z^{\text{nad}} = (-185.89,\ 31.65)$, respectively. All objective values are normalized using these points, and the HV is calculated with the reference point $(1.1,\ 1.1)$. We can clearly see that MFE-NSGA-III achieves a much better HV compared to SA-NSGA-III under the same computational budget of only $T_{\max} = 300$. Figure 8 further illustrates how MFE-NSGA-III attains this performance by selectively evaluating the most important objectives and constraints.

Figure 6 shows the final generation solutions, where three representative solutions A, B, and C are highlighted for detailed electromagnetic analysis. These designs are chosen to represent different trade-offs between average torque (f_1) and torque ripple (f_2). Figure 9 shows the flux distributions for these selected designs. Design A ($f_1 = 204.91,\ f_2 = 26.00$) produces the highest torque but also exhibits increased torque ripple. Design B ($f_1 = 192.37,\ f_2 = 14.58$) achieves a more balanced trade-off with moderate torque and reduced ripple, while Design C ($f_1 = 186.25,\ f_2 = 13.51$) provides the lowest torque but minimal ripple. All three designs exhibit similar emerging patterns of air pockets, with minor variations in the magnet angle, magnet thickness, magnet width, and other related design parameters.

VI. Conclusions

This paper has demonstrated the application of a recently proposed MFE-EMO framework to a computationally expensive electric machine design optimization problem involving three levels of computational fidelity. The study focused on optimizing an interior permanent magnet (IPM) motor for a desirable trade-off between average torque maximization and torque ripple minimization, subject to geometric and structural constraints, involving a heterogeneous range of evaluation times. Automated workflows have been developed in Python to interface with Altair Flux for electromagnetic analysis and Altair SimLab for structural analysis. Two optimization scenarios: one with geometric constraints alone, involving

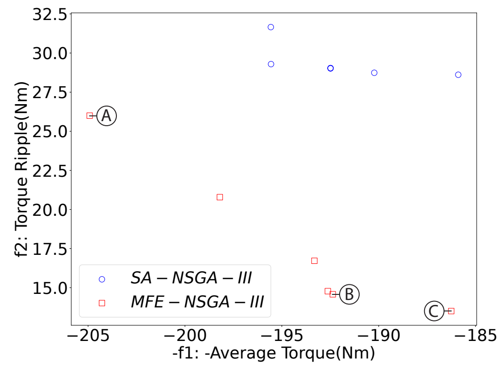

Fig. 6: Obtained final generation feasible Pareto-optimal solutions for both algorithms with ETs ($\boxed{0.43,\ 0.43}\,|\,0.043, 0.043, \dots, 0.043, 0.14$) for the stress-constrained case.

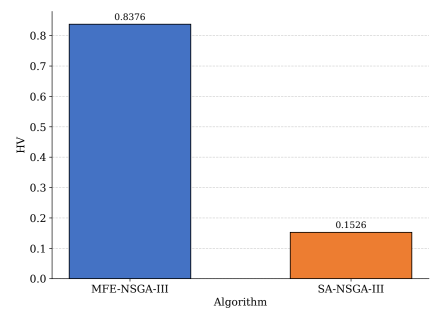

Fig. 7: Comparison of normalized HV values for MFE-NSGA-III and SA-NSGA-III for ET = ($\boxed{0.43,\ 0.43}\,|\,0.043, 0.043, \dots, 0.043, 0.14$) for the stress-constrained case.

two levels of heterogeneity in evaluation times and another with an additional stress constraint, involving three levels of heterogeneity, have been explored.

The results have shown that the proposed MFE-NSGA-III approach efficiently obtains better Pareto-optimal solutions compared to SA-NSGA-III, thereby demonstrating its effectiveness and practicality for real-world engineering design optimization problems involving heterogeneously expensive

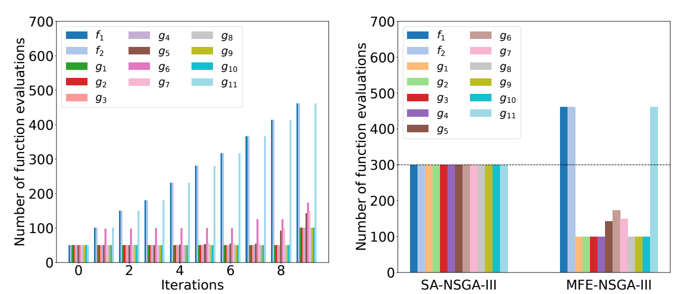

(a) Number of hi-fi evals per iteration for MFE-NSGA-III.

(b) Total no. of hi-fi evals for SA-NSGA-III and MFE-NSGA-III.

Fig. 8: Number of hi-fi evaluations recorded using SA-NSGA-III and MFE-NSGA-III with ETs ($\boxed{0.43,\ 0.43}\,|\,0.043, \dots, 0.043, 0.14$).

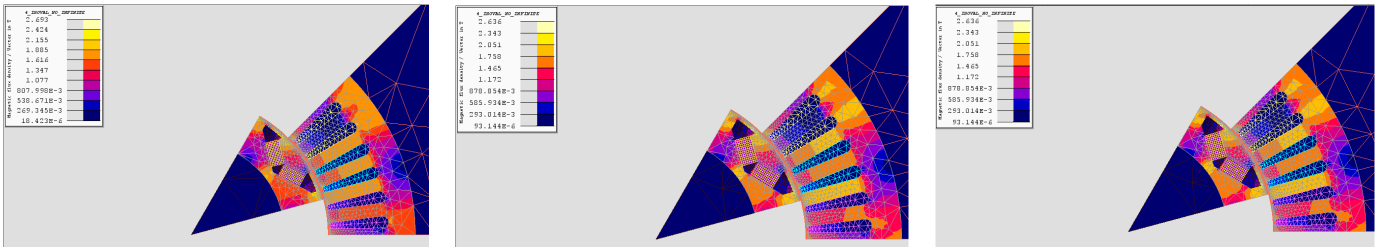

Fig. 9: Flux distributions for three Pareto-optimal designs: A ($f_1 = 204.91,\ f_2 = 26.00$), B ($f_1 = 192.37,\ f_2 = 14.58$), and C ($f_1 = 186.25,\ f_2 = 13.51$).

evaluation times. While a standard surrogate-assisted EMO allocates an identical number of evaluations to all objectives and constraints, irrespective of their evaluation times, MFE-EMO evaluates cheaper, non-dominated, and larger surrogate error objectives/constraints early on and focuses on evaluating expensive objectives/constraints later during an optimization run. As shown, such a flexible and adaptive assignment of evaluation allows more iterations and thereby produces a more effective search.

The proposed MFE-NSGA-III is ready to be applied to other similar practical problems involving heterogeneous evaluation times. Despite the algorithmic novelty, MFE-EMO demonstrates the advantage of using a population of solutions in handling objectives/constraints having heterogeneous evaluation times within an optimization algorithm. A code of the foundational algorithm is available at `https://www.coin-lab.org/content/softwares.html`.

References

[1] I. Boldea and L. N. Tutelea, *Electric machines: steady state, transients, and design with MATLAB*. CRC press, 2009.

[2] J. F. Gieras, *Advancements in electric machines*. Springer Science & Business Media, 2008.

[3] G. Lei, J. Zhu, Y. Guo, C. Liu, and B. Ma, "A review of design optimization methods for electrical machines," *Energies*, vol. 10, no. 12, p. 1962, 2017.

[4] C. Dong, Y. Qian, Y. Zhang, and W. Zhuge, "A review of thermal designs for improving power density in electrical machines," *IEEE Transactions on Transportation Electrification*, vol. 6, no. 4, pp. 1386–1400, 2020.

[5] G. Pellegrino and F. Cupertino, "IPM motor rotor design by means of fea-based multi-objective optimization," in *2010 IEEE International Symposium on Industrial Electronics*, 2010, pp. 1340–1346.

[6] G. Pellegrino, F. Cupertino, and C. Gerada, "Automatic design of synchronous reluctance motors focusing on barrier shape optimization," *IEEE Transactions on Industry Applications*, vol. 51, no. 2, pp. 1465–1474, 2015.

[7] M. Degano, M. Di Nardo, M. Galea, C. Gerada, and D. Gerada, "Global design optimization strategy of a synchronous reluctance machine for light electric vehicles," in *8th IET International Conference on Power Electronics, Machines and Drives (PEMD 2016)*, 2016, pp. 1–5.

[8] S. Ferrari, L. Solimene, R. Torchio, C. Anerdi, F. Freschi, L. Giaccone, G. Lorenti, F. Lucchinizz, P. Alotto, G. Pellegrino, and M. Repetto, "A multiphysics dataset generation procedure for the data-driven modeling of traction electric motors," *IEEE Access*, vol. 13, pp. 54 534–54 546, 2025.

[9] Politecnico di Torino, "Galileo ferraris contest," https://cadema-polito.github.io/GalFer_contest/, accessed: Jan. 20, 2026.

[10] K. Deb, R. Hussein, P. Roy, and G. Toscano, "A taxonomy for metamodeling frameworks for evolutionary multi-objective optimization," *IEEE Transactions on Evolutionary Computation*, vol. 23, no. 1, pp. 104–116, 2019.

[11] K. Deb, P. C. Roy, and R. Hussein, "Surrogate modeling approaches for multiobjective optimization: Methods, taxonomy, and results," *Mathematical and Computational Applications*, vol. 26, no. 1, p. 5, 2020.

[12] T. Chugh, K. Sindhya, J. Hakanen, and K. Miettinen, "A survey on handling computationally expensive multiobjective optimization problems with evolutionary algorithms," *Soft Computing*, vol. 23, pp. 3137–3166, 2019.

[13] Q. Zhang, W. Liu, E. Tsang, and B. Virginas, "Expensive multi-objective optimization by MOEA/D with gaussian process model," *IEEE Transactions on Evolutionary Computation*, vol. 4, no. 3, pp. 456–474, 2010.

[14] K. H. Rahi, H. K. Singh, and T. Ray, "Investigating the use of sequencing and infeasibility driven strategies for constrained optimization," in *2019 IEEE congress on evolutionary computation (CEC)*. Piscataway, NJ, USA: IEEE, 2019, pp. 1642–1649.

[15] T. Chugh, Y. Jin, K. Miettinen, J. Hakanen, and K. Sindhya, "A surrogate-assisted reference vector guided evolutionary algorithm for computationally expensive many-objective optimization," *IEEE Transactions on Evolutionary Computation*, vol. 22, no. 1, pp. 129–142, 2018.

[16] J. Knowles, "ParEGO: A hybrid algorithm with on-line landscap e approximation for expensive multiobjective optimization problems," *IEEE Transactions on Evolutionary Computation*, vol. 10, no. 1, pp. 50–66, 2006.

[17] R. Allmendinger and J. Knowles, "Heterogeneous objectives: State-of-the-art and future research," in *Many-Criteria Optimization and Decision Analysis: State-of-the-Art, Present Challenges, and Future Perspectives*. Cham: Springer, 2023, pp. 317–335.

[18] B. Santoshkumar and K. Deb, "Handling objectives with heterogeneous evaluation times in surrogate-assisted evolutionary multi-objective optimization," *IEEE Transactions on Evolutionary Computation*, pp. 1–1, 2025.

[19] K. Rahi, H. Singh, and T. Ray, "Towards solving expensive optimization problems with heterogeneous constraint costs," in *Proc. of the Genetic and Evol. Comput. Conference Companion*, 2024, pp. 2032–2040.

[20] B. Santoshkumar and K. Deb, "Addressing heterogeneous evaluation times in constrained multi-objective optimization using a mixed-fidelity evaluation technique: Proof-of-concept results," in *Proceedings of the Genetic and Evolutionary Computation Conference*, ser. GECCO '25. New York, NY, USA: Association for Computing Machinery, 2025, p. 645–653.

[21] J. Blank and K. Deb, "Handling constrained multi-objective optimization problems with heterogeneous evaluation times: proof-of-principle results," *Memetic Computing*, vol. 14, no. 2, pp. 135–150, 2022.

[22] B. Santoshkumar and K. Deb, "A mixed-fidelity evaluation algorithm for efficient constrained multi- and many-objective optimization: First results," in *Evolutionary Multi-Criterion Optimization*. Singapore: Springer Nature Singapore, 2025, pp. 147–162.

[23] ——, "Handling of objectives and constraints with heterogeneous evaluation times for surrogate-assisted evolutionary multi- and many-objective optimization," *Swarm and Evolutionary Computation*, vol. 100, p. 102260, 2026.

[24] B. Khoshoo, J. Blank, T. Q. Pham, K. Deb, and S. N. Foster, "Optimal design of electric machine with efficient handling of constraints and surrogate assistance," *Engineering Optimization*, vol. 56, no. 2, pp. 274–292, 2024.

[25] Altair Engineering Inc., *Altair Flux*, 2023, altair Flux (Version 2023.1). Altair Engineering Inc. https://www.altair.com/flux/.

[26] ——, *Altair SimLab*, 2022, altair SimLab (Version 2022.3). Altair Engineering Inc. https://www.altair.com/simlab/.